Calculation of Temperature Rise in Air-cooled Induction Motors Through 3-D Coupled Electromagnetic Fluid-Dynamical and Thermal Finite-Element Analysis

Yujiao ZHANG, Jiangjun RUAN, Tao HUANG, and Xiaoping YANG

School of Electrical Engineering, Wuhan University, 430072, China
jiao_zyj@163.com

Abstract —This paper investigates a 3-D coupled-field finite-element method (FEM) used in the simulation of the temperature distribution in air-cooled asynchronous induction motors. The temperature rise in motor is due to Joule's losses in stator windings and the induced eddy current in squirrel cages, and heat dissipation by air convection and solid conduction. The Joule's losses calculated by 3-D eddy- current field analysis are used as the input for the thermal field analysis, which is deeply dependent on accurate air fluid field analysis. A novel multicomponent fluid model is proposed to deal with the influence of rotor rotation upon the air convection. A test prototype is designed and manufactured. The good agreement of the temperature distributions between simulated and measured results validates the proposed methodology.

I. INTRODUCTION

The ventilation system design of air-cooled induction motors is a complex task that must determine the thermal loads to achieve the maximum insulation material exploitation [1]. An optimal design is a multi-physical coupled process that involves electromagnetic losses as well as fluid dynamic and thermal behavior. Moreover, a key problem in the thermal analysis of induction motors is the complexity of air courses and the influence of rotation upon air convection, which cannot be accurately evaluated by using traditional equivalent lumped circuits together with empirical curves method. Therefore, a coupled analysis of eddy-current, fluid and thermal fields is mandatory to compute the temperature rise in the design stage [2].

The rotor parts produce a fan action. Therefore, the influence of centrifugal force and Coriolis force caused by rotation upon air convection in the air gap must be considered [2]. However, according to no-slip boundary condition in fluid dynamic theory, rotation velocity on interface between air gap and rotor cannot be applied directly. To deal with this problem in fluid field analysis, we propose a novel multicomponent fluid model, in which all rotor parts are taken as fluids under some constraint conditions.

In addition, in this paper, magnetic saturation and nonlinear resistivity with temperature are also taken into account. A 6-phase 8-pole 200kW asynchronous motor as a test prototype is designed and manufactured to verify the proposed methodology. A good agreement of the temperature distributions are achieved between simulated and measured results.

II. FORMULATION

The flowchart of the entire analytical methodology is shown in Fig. 1. Starting from the 3-D FEM model of a motor, eddy-current and fluid simulations are carried out to obtain the losses of every element and air-flow velocity of every node. The thermal computation is tightly coupled to the electro-magnetic and fluid-dynamical results. The resistivity of stator windings and squirrel cage is updated in accordance to the thermal field calculation result until the difference of temperature between two adjacent steps is less than 0.01℃.

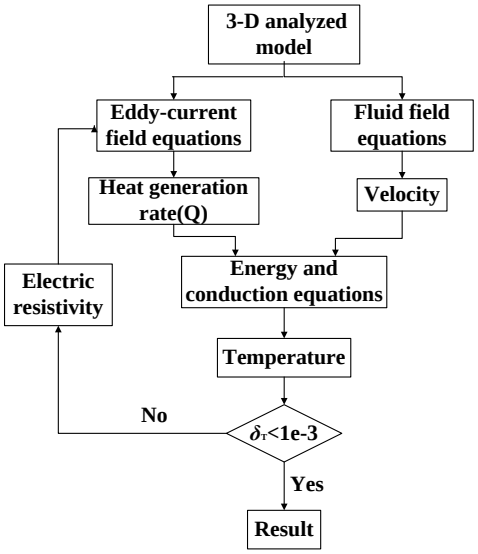

Fig. 1. The flowchart of the entire analytical methodology.

Under above restrictions, the fluid equations of rotor components can be simplified as:

$$\frac{\partial \upsilon_\theta}{\partial \theta} = 0, \upsilon_\theta = \omega r \tag{1}$$

$$-\rho_2 \frac{\upsilon_\theta^2}{r} = -\frac{\partial p}{\partial r} \tag{2}$$

$$0 = \frac{\partial}{\partial r}\left[\frac{1}{r}\frac{\partial}{\partial r}(r\upsilon_\theta)\right] \tag{3}$$

where ρ_2 is the actual density of rotating components. Obviously, viscosity coefficient doesn't affect the results.

III. CALCULATIONS OF A 6-PHASE MOTOR

A 6-phase 8-pole 200kW asynchronous motor as a test prototype has been designed and manufactured Fig. 2 shows the 3-D computed model. Although the influence of end windings cannot be ignored, because of the complexity

of its structure and large amount of computation, it wasn't considered temporarily in this study stage. The model is meshed with prism-shaped elements. There are 1,287,061 elements and 534,703 nodes.

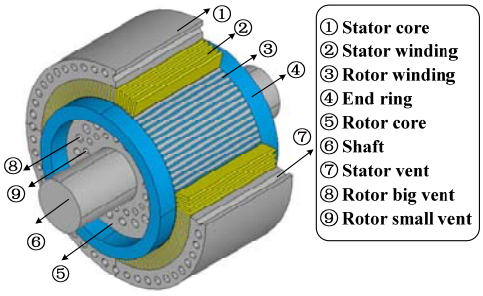

Fig. 2. Cross-sectional view of 6-phase motor.

In the computation of the eddy-current field, the rated source current is 110.6 A. The rated frequency of current in stator windings is 30.78 Hz. Considering the influence of rotor rotation, the frequency (f) is converted into $f \times s$ (s is the slip.). In the computation of the fluid and thermal field, actual measured wind velocity condition is applied to inlet boundary, and pressure on outlet boundary is defined as a standard atmospheric pressure. The rated rotational speed was applied to rotor and shaft. Considering the low conductivity of insulation material, the thermal conductivity of stator windings is anisotropic. The ambient temperature is set to 20℃.

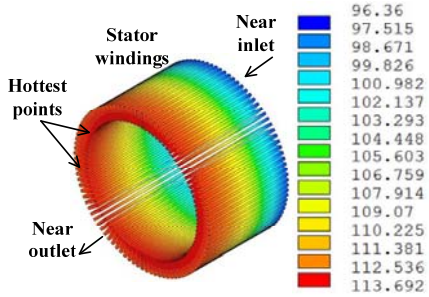

Fig. 3. Temperature distribution of stator windings.

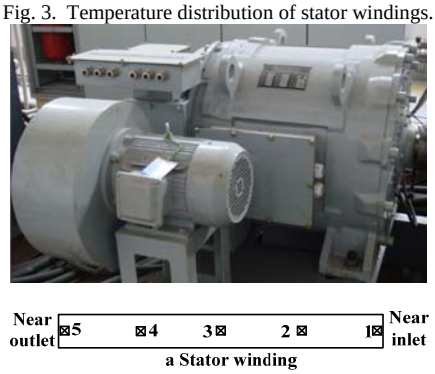

Fig. 4. Experimental system. (a) Picture of the prototype. (b) Measured points along a stator winding

IV. EXPERIMENTAL VERIFICATION

In order to check whether the simulations complies with the actual situation, an experimental system is built and tested as shown in Fig. 4(a). In the test, the temperature of five points along an axial stator winding is measured (measurement positions are as shown in Fig. 4(b)). The temperature measurements are taken using thermocouples. After three hours' operating, we got the results of the test, which indicate that the temperature rise in the measured points on the stator winding is in good agreement with the computed result. Table I gives the tested and computed temperature rise results. Close agreement between the computed and measured temperature rises can be seen as a good validation of the proposed methodology.

TABLE I
TESTED AND CALCULATED OF TEMPERATURE RISE (℃)

Measured point	Tested	Computed	Error (%)
1	80.8	87.332	8.1
2	84.5	89.010	5.3
3	90.0	91.633	1.8
4	95.6	93.102	-2.6
5	100.9	93.660	-7.2

Obviously, the end windings is one of the main factors influencing the thermal performance of motor, because the wind blows to the end windings directly, which facilitates the cooling of it. Indeed, near the inlet of the cooling air, due to the cooling effect, the temperature rise tested is lower than the value computed, but it is higher than the value computed near the outlet of the air.

V. CONCLUSION

This paper proposes a 3-D coupled-field analysis to predict the temperature rise in air-cooled induction motors. Furthermore, the multiple species of fluids analysis is presented to consider the influence of rotation upon air-flow in air gap. To validate the coupled-field analysis presented in this paper, calculated results are compared with tested data. It's found to be in good agreement. The consideration of nonlinear properties of material will be expected to produce better results.

VI. REFERENCES

[1] M. Farahani, et al., "Behavior of Machine Insulation Systems Subjected to Accelerated Thermal Aging Test," *IEEE Transactions on Dielectrics and Electrical Insulation,* vol. 17, pp. 1364-1372, Oct 2010.

[2] F. Marignetti, et al., "Design of Axial Flux PM Synchronous Machines Through 3-D Coupled Electromagnetic Thermal and Fluid-Dynamical Finite-Element Analysis," *IEEE Transactions on Industrial Electronics,* vol. 55, pp. 3591-3601, Oct 2008.

[3] W. N. Fu, et al., "A Finite Element Method for Transient Analysis of Power Electronic Motor Drives Including Parasitic Capacitive Effect and External Circuit," *2008 IEEE International Symposium on Electromagnetic Compatibility,* vols 1-3, pp. 108-113, 2008.

[4] E. Dlala and A. Arkkio, "A General Model for Investigating the Effects of the Frequency Converter on the Magnetic Iron Losses of a Squirrel-Cage Induction Motor," *IEEE Transactions on Magnetics,* vol. 45, pp. 3303-3315, Sep 2009.

[5] M. J. Islam, et al., "Eddy-Current Loss and Temperature Rise in the Form-Wound Stator Winding of an Inverter-Fed Cage Induction Motor," *IEEE Transactions on Magnetics,* vol. 46, pp. 3413-3416, Aug 2010.

[6] H. Kurose, et al., "3-D Eddy Current Analysis of Induction Heating Apparatus Considering Heat Emission, Heat Conduction, and Temperature Dependence of Magnetic Characteristics," *IEEE Transactions on Magnetics,* vol. 45, pp. 1847-1850, Mar 2009.

[7] S. Mezani, et al., "A combined electromagnetic and thermal analysis of induction motors," *IEEE Transactions on Magnetics,* vol. 41, pp. 1572-1575, May 2005.